Observation of a Half Step Magnetization in the $\{Cu_3\}$-Type Triangular Spin Ring

Kwang-Yong Choi,[1] Yasuhiro H. Matsuda,[2] and Hiroyuki Nojiri[1]

[1]*Institute for Materials Research, Tohoku University, Katahira 2-1-1, Sendai 980-8577, Japan, and CREST, Japan Science and Technology Agency, Japan*

[2]*Department of Physics, Okayama University, Okayama 700-8530, Japan*

U. Kortz,[3] F. Hussain,[3] Ashley C. Stowe,[4] Chris Ramsey,[4] and Naresh S. Dalal[4]

[3]*School of Engineering and Science, International University of Bremen, P.O. Box 750 561, 28725 Bremen, Germany*

[4]*Department of Chemistry and Biochemistry, Florida State University and National High Magnetic Field Laboratory, Tallahassee, Florida 32306-4390, USA*

(Received 18 August 2005; published 13 March 2006)

We report pulsed field magnetization and ESR experiments on a $\{Cu_3\}$ nanomagnet, where antiferromagnetically coupled Cu^{2+} ($S = 1/2$) ions form a slightly distorted triangle. The remarkable feature is the observation of a half step magnetization, hysteresis loops, and an asymmetric magnetization between a positive and a negative field in a fast sweeping external field. This is attributed to an adiabatic change of magnetization. The energy levels determined by ESR unveil that the different mixing nature of a spin chirality of a total $S = 1/2$ Kramers doublet by virtue of Dzyaloshinskii-Moriya interactions is decisive for inducing half step magnetization.

DOI: 10.1103/PhysRevLett.96.107202 PACS numbers: 75.50.Xx, 75.45.+j, 75.60.Ej, 76.30.−v

In recent years, nanosized molecular magnets have been intensively explored due to pronounced quantum phenomena [1–3]. Often, however, quantum effects are obscured by environments (''heat bath'' via spins and phonons) leading to decoherence and thermal relaxations. A promising way to quench environments is to exploit a fast sweeping pulsed magnetic field [4]. Moreover, one can differentiate a pure quantum magnetization from an isothermal one by adopting a unique spin topology and sizable anisotropic exchange interactions [5,6]. $S = 1/2$ antiferromagnetic triangular spin rings might be the best candidate to observe peculiar quantum magnetization owing to two doublets with a different spin chirality [7–9]. To our knowledge, such an issue has been addressed in a V_3 complex [7]. However, the use of powders and large thermal effects prevent the unveiling of a full aspect of magnetization. We have now used single crystals of a new class of materials which enable us, for the first time, to provide clear-cut evidence for the much sought-after half step magnetization.

$Na_9[Cu_3Na_3(H_2O)_9(\alpha\text{-}AsW_9O_{33})_2] \cdot 26\ H_2O$ (hereafter abbreviated as $\{Cu_3\}$) realizes the triangle nanomagnet [10–12]. As Fig. 1(a) displays, it has a sandwich-type structure with D_{3h} symmetry [12]. The central belt, separated by two $[\alpha\text{-}AsW_9O_{33}]^{9-}$ subunits, consists of three $CuO_4(H_2O)$ square pyramids linked by Na^+ ions. In the unit cell, there are two triangle spin rings of Cu^{2+} ions. Figure 1(b) is a zoom of local coordinations of the copper ions. They possess two different local bonding length and angles: Cu(1)-O (1.909–1.949 Å) and O-Cu(1)-O (88.9°–90.5°) and Cu(2)-O (1.912–1.918 Å) and O-Cu(2)-O (89.1°–90.4°). Since the superexchange path between each copper ion (Cu-O-W-O-W-O-Cu) is identical, the $\{Cu_3\}$ nanomagnet can be regarded as an $S = 1/2$ triangle spin ring. Static susceptibility shows that the Cu^{2+} ions are antiferromagnetically coupled [10].

In this Letter, we report dynamic magnetization processes such as a half step magnetization, hysteresis loops, and an asymmetric magnetization between a positive and a negative field on the $\{Cu_3\}$-triangle spin ring. This feature is characteristic for an adiabatic change of magnetization. We will demonstrate that a spin chirality and Dzyaloshinskii-Moriya (DM) interactions are an essential ingredient to observe a half step magnetization.

The preparation of single crystals is described in Ref. [12]. Magnetization measurements were carried out

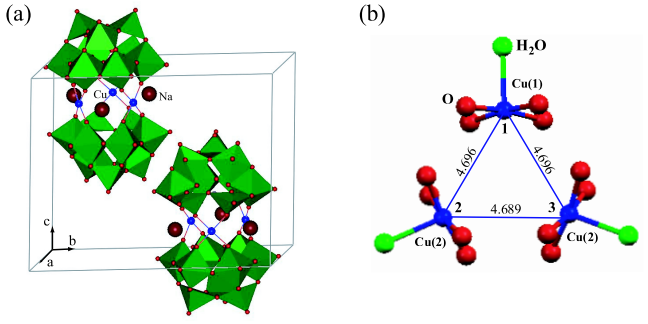

FIG. 1 (color online). (a) The crystal structure of the Cu_3-triangle spin ring. For clarity, only the copper (medium blue balls), the sodium (large purple balls), and the oxygen (small red balls) ions are shown. (b) A zoom of three Cu^{2+} ions with local coordinations. The solid lines are a connection between the nearest Cu^{2+} ions. The numbers represent $Cu \cdots Cu$ distances; $Cu_1 \cdots Cu_2 = Cu_1 \cdots Cu_3 = 4.696$ Å and $Cu_2 \cdots Cu_3 = 4.689$ Å.

by means of a standard inductive method. Fast pulsed magnetic fields up to 10^3 T/s were generated by a capacitor bank of 90 kJ as described elsewhere [4]. The sample is immersed in liquid ^{3}He to reach a temperature as low as 0.4 K. ESR measurements were performed using a commercial Bruker spectrometer at the Q band ($\nu \approx 34$ GHz).

Shown in Fig. 2 is the magnetization versus magnetic field at 0.4 K for the H $\parallel$ plane. Upon sweeping the pulsed field upwardly ($A \rightarrow B$), the magnetization first shows a plateau around $1.15\mu_B$, then jumps to $2.6\mu_B$, and finally approaches gradually to the saturation value of $3.4\mu_B$ in a high field of 13 T. Here note that the magnetization is renormalized by the g factor of $g = 2.25$ (see below). Thus, the observed jumps correspond to $ngS\mu_B$ ($n = 1, 2, 3$). In the down sweep after saturation ($B \rightarrow C$), the magnetization exhibits a sharp drop first from $3.4\mu_B$ to $1.15\mu_B$ and then to zero. Remarkably, the contrasting magnetization between the up and down sweeps leads to pronounced hysteresis loops, which are unusual for Cu^{2+} ions with no single ion anisotropy. To gain more insight, we have calculated the magnetization at equilibrium denoted by the thin line. We can identify the first step to the saturation of $S^T = 1/2$ state. The second step by $2.25\mu_B$ comes from the level crossing fields between $S^T = 1/2$ and $S^T = 3/2$ states.

A close inspection reveals that the up sweep magnetization is smaller than the equilibrium one in low fields of 0–2.3 T. At high fields of 5–8 T, the second step magnetization of $1.45\mu_B$ amounts to nearly half of the equilibrium value. In the down sweep, a half step magnetization is totally missing while the magnetization jumps become more sharp than the equilibrium one. This implies that the effective temperature of the spin system is lower than that at equilibrium. Therefore, this strongly suggests that the fast sweeping field decouples the spin system from environments and the anomalous magnetization relies on a pure quantum mechanical process.

The distinct behavior is further highlighted by the magnetization in a negative field. It exhibits neither half step magnetization nor pronounced hysteresis. Both the up and down sweep magnetizations show a successive, sharp step first to $-1.4\mu_B$ and then to $-3.4\mu_B$. To figure out a full aspect of the anomalous magnetization behavior, first of all, an energy level diagram and crossing point should be precisely determined [5]. An extremely high sensitivity of ESR on anisotropic exchange interactions can serve as an experimental choice.

In Fig. 3(a), the representative ESR spectra at 8.8 K are compared between 0° and 90°. The angle is measured starting from the molecular C_3 axis, which is perpendicular to the plane comprising the three copper ions. The intense three lines originate from the excited $S^T = 3/2$ group. For the assignment of the respective transitions, refer to Figs. 3(a) and 4. In addition, we are able to resolve the transitions arising from the $S^T = 1/2$ group. The ESR intensity of the $S^T = 1/2$ group is comparable to each other and is 1 order of magnitude weaker than that of the $S^T = 3/2$ group. This is due to the reduced magnitude of spin. The transitions of $|1\rangle \rightarrow |3\rangle$ and $|2\rangle \rightarrow |4\rangle$ are conventional ESR transitions between the Zeeman splitting

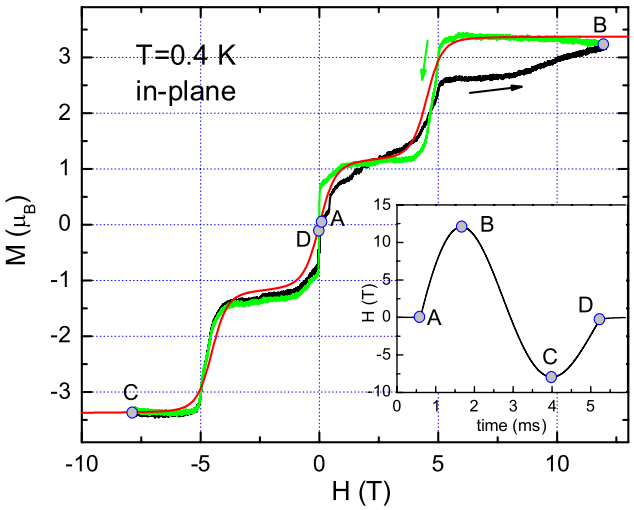

FIG. 2 (color online). Magnetization curve vs pulsed magnetic field at 0.4 K. The saturated magnetization is scaled to $g\mu_B S$. The thin line is the calculated isothermal magnetization curve. Arrows denote sweep directions ($A \rightarrow B \rightarrow C \rightarrow D$). The inset shows the pulsed magnetic field versus time.

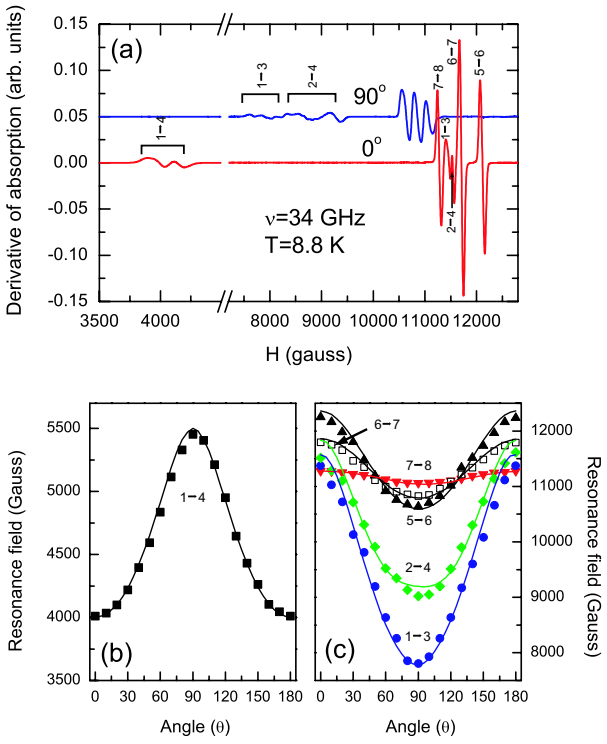

FIG. 3 (color online). (a) Representative ESR spectrum at 8.8 K. The numbers denote the ESR transitions between the energy levels marked in Fig. 4. (b),(c) Angle dependence of the ESR spectrum at 8.8 K. The solid lines are the calculated curves.

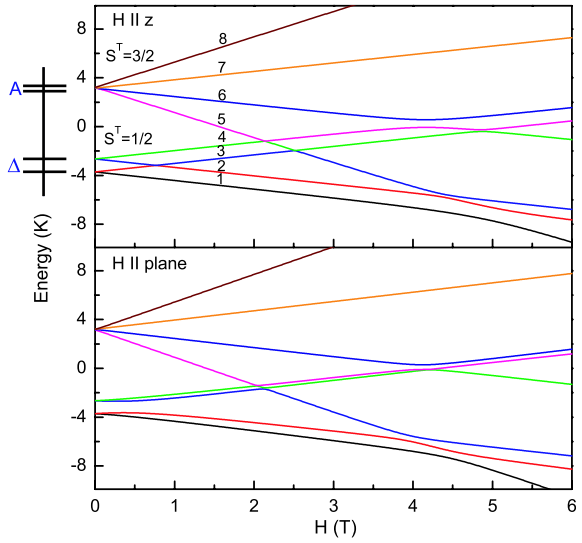

FIG. 4 (color online). Energy level diagrams for the Hamiltonian of Eq. (1) for a magnetic field parallel and perpendicular to the plane, respectively. For the fitting parameters, see the text.

states. In addition, there appear symmetry-forbidden transitions of $|1\rangle \rightarrow |4\rangle$ and $|2\rangle \rightarrow |3\rangle$. The rest of the transitions $|1\rangle \rightarrow |2\rangle$ and $|3\rangle \rightarrow |4\rangle$ are out of resonance in the Q band regime.

Noticeably, each spectrum of the $S^T = 1/2$ group has a fine structure. The uniform angular dependence indicates that it is intrinsic rather than due to defects. Anisotropic interactions are sensitive to local distortions of $CuO_4(H_2O)$ square pyramids, which have a strong impact on the energy levels of the $S^T = 1/2$ group. Thus, the Jahn-Teller isomerism is likely to be responsible for that. For the studied $\{Cu_3\}$ nanomagnet, however, the magnetic properties are not significantly influenced by the isomers for the following reasons. First, the magnetization and ESR spectra show no substantial sample dependence (not shown here). Second, the observation of only the three signals from the $S^T = 3/2$ group implies that the variance between the isomers is tiny. Actually, our simulations restrict the deviations of anisotropic interactions to only a few percent among the isomers. The details will be published elsewhere [13]. Hereafter, we will focus on the main configuration, yielding the most intense signals.

Figures 3(b) and 3(c) display the angular dependence of the resonance fields at 8.8 K. The experimental spectra are fitted to a sum of a Gaussian profile using a least-squares method. Error bars of the fitted data are within the size of the symbols. The resonance fields of the $S^T = 1/2$ group vary strongly with an angle with respect to the $S^T = 3/2$ group. In particular, the unconventional ESR transition of $|1\rangle \rightarrow |4\rangle$ shows an angular dependence opposite to the conventional ones.

Based on these data, we will determine the magnetic parameters of a $S = 1/2$ Hamiltonian of the $\{Cu_3\}$-triangle spin ring external field as follows:

$$\mathcal{H} = \sum_{l=1}^{3} \sum_{\alpha=x,y,z} J^{\alpha}_{ll+1} \mathbf{S}_l \cdot \mathbf{S}_{l+1} + \sum_{l=1}^{3} \mathbf{D}_{ll+1} \cdot [\mathbf{S}_l \times \mathbf{S}_{l+1}] + \mu_B \sum_{l=1}^{3} \mathbf{S}_l \cdot \tilde{\mathbf{g}}_{ll} \cdot \mathbf{H}_l, \quad (1)$$

where the exchange coupling constants J^{α}_{ll+1}, the DM vectors $\mathbf{D}_{ll+1}$, and the g tensors $\tilde{\mathbf{g}}_{ll}$ are defined as a site-dependent quantity with a periodic boundary condition.

First, the g factors are determined using ESR data; $g^{xx}_{11} = g^{yy}_{11} = 2.2(5)$, $g^{xx}_{22} = g^{yy}_{22} = 2.1(0)$, $g^{xx}_{33} = g^{yy}_{33} = 2.4(0)$, and $g^{zz}_{ii} = 2.0(6)$ ($i = 1$, 2, and 3). Note that the average g value of $g^{xx}_{\mathrm{av}} = g^{yy}_{\mathrm{av}} = 2.25$ and $g^{zz}_{\mathrm{av}} = 2.06$ is typical for the $CuO_4(H_2O)$ square pyramids having $3d_{x^2-y^2}$ orbitals [14]. Second, J^{α}_{ll+1} is decided by the magnetization measurements along the H $\perp$ plane and the H $\parallel$ plane. J^{α}_{ll+1} is restricted to satisfy an isosceles triangle condition. We obtain $J^x_{12} = J^y_{12} = 4.50(0)$ K, $J^z_{12} = 4.56(0)$ K, $J^x_{23} = J^y_{23} = J^x_{31} = J^y_{31} = 4.03(0)$ K, and $J^z_{23} = J^z_{31} = 4.06(0)$ K. The symmetric anisotropic exchange interactions, amounting to 1% of J^z_{ij}, are introduced by considering a crystal structure and are adjusted by the angular dependence of ESR and the splitting of the $S^T = 3/2$ multiplet. The final step is to determine DM interactions, which are allowed due to a slight distortion of the $\{Cu_3\}$ triangle. There are six DM vectors to be fixed in the two spin triangles. If one of them is known, say, $\mathbf{D}_{12}$, the rest will be obtained by applying the D_{3h} symmetry operation. Note that the z component of the DM vectors is identical for all sites. The in-plane component obeys approximately C_3 symmetry; $(D^x_{23}, D^y_{23}) = \mathcal{R}(2\pi/3) \times (D^x_{12}, D^y_{12})$ and $(D^x_{31}, D^y_{31}) = \mathcal{R}(4\pi/3)(D^x_{12}, D^y_{12})$, where $\mathcal{R}(\theta)$ denotes a rotation of the triangle by θ. The DM vectors between two spin triangles are transformed as $\mathbf{D}'_{ll+1} = \sigma_h \mathbf{D}_{ll+1}$, where σ_h is a reflection about a horizontal plane. A fitting to the angular dependence of the resonance fields yields $D^x_{12} = D^y_{12} = D^z_{12} = 0.52(9)$ K. The DM interactions amount to 12% of J^z_{ij}, which is a typical order of magnitude for Cu^{2+} spin systems. Here we stress that the parameters are uniquely determined by the magnetization and ESR measurements as well as by symmetry considerations.

Our result is consistent with an earlier study [10]. In Ref. [10], ESR spectra were analyzed in terms of the spin Hamiltonian defined using a zero-field splitting parameter D. At zero field, the energy splitting within the $S^T = 3/2$ state is given by $2D = 0.066(2)$ K [10]. In our model, this corresponds to the exchange anisotropy $A = |J^x - J^z| \sim 0.6$ K, which induces the zero-field gap of 0.0683(4) K (see Fig. 4). In contrast to our microscopic model, however, the effective spin Hamiltonian cannot account for the detailed ESR features of the $S^T = 1/2$ state ($D = 0$).

Shown in Fig. 4 is the resulting energy level diagram. At zero field, the energy gap of $\Delta = 1.0(6)$ K opens between

a Kramers and a second degenerate doublet. This is larger than the estimated value from the isosceles triangle condition of J_{12}–$J_{23} = 0.5$ K. The remaining energy splitting is provided by the DM interactions of 0.52(9) K. For the H $\perp$ plane (H $\parallel z$), there are the two level repulsions at $H_{c_1} = 4.4$ T and $H_{c_2} = 5$ T. For the H $\parallel$ plane, the two level repulsions occur at slightly lower fields of $H_{c_1} = 3.9$ T and $H_{c_2} = 4.4$ T. Besides, there are additional antilevel crossings around 0.4 and 2.1 T. The level crossing points match well with the fields at which the step magnetization by $2.25\mu_B$ is observed. In the following, we will address the detailed behavior of the dynamic magnetization.

At zero field, the relative population between the $S_z^T = -1/2$ and the $S_z^T = +1/2$ levels is given by the ratio of $1{:}e^{-\Delta/k_BT} \approx 1{:}0.72$, with the energy gap of $\Delta = 1.0(6)$ K. When a sweeping of magnetic field is faster than the relaxation time between the two states (actually, this is our case), the nonadiabatic transition will increase the population of the $S_z^T = +1/2$ state with respect to the thermal equilibrium state. This leads to a reduction of magnetization compared to the equilibrium value (see the up sweep magnetization of Fig. 2).

Next, we turn to the nearly half step magnetization at high fields between 5–8 T in the up sweep. As Fig. 4 shows, for the up sweep the lowest $S^T = 1/2$ state transits to the lowest $S^T = 3/2$ one. In contrast, the second lowest $S^T = 1/2$ state follows the successive transition of $S^T = 1/2 \rightarrow S^T = 3/2 \rightarrow S^T = 1/2$. Thus, the former process will contribute to the magnetization by $2.25\mu_B$, while the latter will give zero magnetization above 4.6 T. When the two processes are averaged, we expect the half step magnetization of $1.125\mu_B$ at zero temperature. The observed step of $1.45\mu_B$ is slightly bigger than the expected value due to the sizable zero-field splitting between the two doublets. Namely, the number of spins in the lowest level is larger than 50%. We recall that the ground state of a perfect triangle is characterized by a total spin $S^T = 1/2$ with a degenerated chirality (''pseudospin 1/2''). DM interactions lift a degeneracy and lead to a different behavior of level crossings between the $S^T = 1/2$ and $S^T = 3/2$ states; the ground state has an antilevel crossing with the $S^T = 3/2$ state, while the second lowest state shows a tiny admixture to it. This indicates that the ground state has dominantly a left chirality and the half step magnetization arises from a different mixing nature of the spin chirality states to the $S^T = 3/2$ states.

Above 8 T, the magnetization gradually approaches to the equilibrium value of $3.4\mu_B$. The field sweep speed dH/dt follows a cosine-type time dependence (see the inset in Fig. 2). When approaching to the point B, thus, dH/dt goes to zero. In this situation, we expect that, at some high field, the sweep field period will slow down to the extent that the second lowest $S^T = 1/2$ state undergoes a relaxation to the lowest $S^T = 3/2$ one. Therefore, the increasing magnetization to the saturation value above 8 T implies that the nonequilibrium magnetization process is switched to the equilibrium one.

As a result, in the down sweep after saturation, all spins are mostly occupied in the lowest $S^T = 3/2$ state. Thus, the magnetization process is exclusively governed by the transition from the lowest $S^T = 3/2$ state to the lowest $S^T = 1/2$ one. Since the spins are mostly confined to the ground state, the effective temperature of the spin system is much lower than the equilibrium one. Actually, the sharp drop of the magnetization with a larger value than equilibrium state confirms this. Therefore, we conclude that the hysteresis loop results from the competition between the fast sweeping field and the thermal relaxation.

Upon sweeping toward a negative field, the lowest $S^T = 1/2$ state transits to the excited $S^T = 1/2$ one. The latter undergoes a transition to the lowest $S^T = 3/2$ state around -2 T. This yields an additional contribution to the magnetization and is fully consistent with the enhanced magnetization of $-1.4\mu_B$ between -2 and -4 T, compared to the equilibrium value.

In conclusion, we have reported the observation of a nearly half step magnetization, hysteresis loops, and an asymmetric magnetization between a positive and a negative field in the $\{Cu_3\}$-triangular spin ring. This is ascribed to an adiabatic magnetization process, relying on the mixing symmetry of the energy levels in the $S = 1/2$ triangular spin ring. Our study suggests that in frustrated spin systems a spin chirality is an essential parameter in realizing a nanoscale storing device.

We thank S. Miyashita and H. De Raedt for valuable discussions. This work was partly supported by a Grant-in-Aid for Scientific Research on Priority Areas from the Ministry of Education, Culture, Sports, Science and Technology, and by NSF, NIRT Grant No. 0103290.

[1] L. Gunther and B. Barbara, *Quantum Tunneling of Magnetization* (Kluwer Academic, Dordrecht, 1995).
[2] L. Thomas *et al.*, Nature (London) **383**, 145 (1996).
[3] W. Wernsdorfer and R. Sessoli, Science **284**, 133 (1999).
[4] H. Nojiri *et al.*, Physica (Amsterdam) **346B–347B**, 216 (2004).
[5] S. Miyashita and N. Nagaosa, Prog. Theor. Phys. **106**, 533 (2001).
[6] S. Miyashita *et al.*, Prog. Theor. Phys. Suppl. **145**, 370 (2002).
[7] T. Yamase *et al.*, Inorg. Chem. **43**, 8150 (2004).
[8] H. De Raedt *et al.*, Phys. Status Solidi B **241**, 1180 (2004).
[9] H. De Raedt *et al.*, Phys. Rev. B **70**, 064401 (2004).
[10] U. Kortz *et al.*, Inorg. Chem. **43**, 144 (2004).
[11] A. C. Stowe *et al.*, Eur. J. Inorg. Chem. 19 (2004) 3792.
[12] U. Kortz *et al.*, Inorg. Chem. **40**, 4742 (2001).
[13] K.-Y. Choi and H. Nojiri (unpublished).
[14] A. Abragam and B. Bleaney, *Electron Paramagnetic Resonance of Transition Ions* (Dover, New York, 1970).